Applied Geochemistry 62 (2015) 3–17

Contents lists available at ScienceDirect

Applied Geochemistry

journal homepage: www.elsevier.com/locate/apgeochem

Arsenic and antimony geochemistry of mine wastes, associated waters and sediments at the Giant Mine, Yellowknife, Northwest Territories, Canada

Skya E. Fawcett[a], Heather E. Jamieson[a,*], D. Kirk Nordstrom[b], R. Blaine McCleskey[b]

[a] Department of Geological Sciences and Geological Engineering, Queen's University, Kingston, ON K7L 3N6, Canada
[b] U.S. Geological Survey, 3215 Marine St., Boulder, CO 80303-1066, USA

ARTICLE INFO

Article history:
Available online 8 January 2015

ABSTRACT

Elevated levels of arsenic (As) and antimony (Sb) in water and sediments are legacy residues found downstream from gold-mining activities at the Giant Mine in Yellowknife, Northwest Territories (NWT), Canada. To track the transport and fate of As and Sb, samples of mine-waste from the mill, and surface water, sediment, pore-water, and vegetation downstream of the mine were collected. Mine waste, pore-water, and sediment samples were analyzed for bulk chemistry, and aqueous and solid-state speciation. Sediment and vegetation chemistry were evaluated using scanning electron microscope imaging, synchrotron-based element mapping and electron microprobe analysis. The distributions of As and Sb in sediments were similar, yet their distributions in the corresponding pore-waters were mostly dissimilar, and the mobility of As was greater than that of Sb. Competition for sorption sites is the most likely cause of elevated Sb concentrations in relatively oxidized pore-water and surface water. The aqueous and solid-state speciation of As and Sb also differed. In pore-water, As(V) dominated in oxidizing environments and As(III) in reducing environments. In contrast, the Sb(V) species dominated in all but one pore-water sample, even under reducing conditions. Antimony(III) appears to preferentially precipitate or adsorb onto sulfides as evidenced by the prevalence of an Sb(III)-S secondary solid-phase and the lack of Sb(III)(aq) in the deeper zones. The As(V)–O solid phase became depleted with depth below the sediment–water interface, and the Sb(V)–O phase persisted under relatively reducing conditions. In the surficial zone at a site populated by *Equisetum fluviatile* (common horsetail), As and Sb were associated with organic material and appeared mobile in the root zone. In the zone below active plant growth, As and Sb were associated primarily with inorganic phases suggesting a release and reprecipitation of these elements upon plant death. The co-existence of reduced and oxidized As and Sb species, instability of some phases under changing redox conditions, and plant uptake and release pose challenges for remediation efforts at the mine.

1. Introduction

The mobility, attenuation, and transformation mechanisms of metal(loid)s in the environment is important for understanding and evaluating the potential risks to ecosystems and humans, for predicting their stability over time, and for designing effective remediation strategies of contaminated sites. Arsenic and Sb are in the same group in the periodic table, have similar electronic structures (ns^2p^3), and are strongly associated in some hydrothermal mineral deposits. For these reasons it is often assumed that they exhibit similar geochemical behavior. Research conducted at the Giant Mine, a former gold mine in Yellowknife, NWT, Canada (Fig. 1) offered an opportunity to compare the geochemical behavior of As and Sb because both elements are elevated in mine waste and in the surrounding environment. Ore was roasted at Giant to extract gold, resulting in a complex range of solid As and Sb-bearing phases in the mine waste. Also, a water treatment plant has been operating at the site for 17 years before sampling, influencing the speciation of metalloids downstream in Baker Pond and Baker Creek. Determining the fate of As and Sb in the environment requires an understanding of the effects of anthropogenic processing on speciation as well as identification of the major controls on As and Sb mobility and speciation under different natural environmental conditions. An understanding of the mobility and possible attenuation of As and Sb is important because Baker Creek is the main conduit for mine waste into Yellowknife Bay (Fig. 2). The aim of this study was to determine the distribution and speciation

---

[*] Corresponding author. Tel.: +1 613 533 6181; fax: +1 613 533 6592.
E-mail address: jamieson@queensu.ca (H.E. Jamieson).

http://dx.doi.org/10.1016/j.apgeochem.2014.12.012
0883-2927/

of As and Sb throughout the paths taken by these contaminants, from the roaster at the mine through water bodies, sediments, and vegetation, and to infer the processes that control the mobility and attenuation of these two elements.

1.1. Mobility and attenuation of As and Sb

The oxide minerals of As and Sb are highly soluble (Greenwood and Earnshaw, 1984), so it is only at very high concentrations of these elements that pure As and Sb oxides are expected to control the activities of As and Sb in solution. Concentrations can be attenuated by sorption to Fe and Mn oxides and oxyhydroxides (Ackermann et al., 2008; Kneebone et al., 2002; Leuz et al., 2006a; Manning et al., 1998; Martinez-Llado et al., 2008; Mitsunobu et al., 2006; Morin et al., 1999; Scheinost et al., 2006; Takahashi et al., 2010; Waychunas et al., 1993), although the strength of those bonds differs for the various species. For example, Sb(III) strongly adsorbs to goethite over a much wider pH range (3–12) and forms the stronger bonds, compared to Sb(V) (Leuz et al., 2006a). In contrast, As(V) binds more strongly and over a lower pH range on the surfaces of iron oxide minerals than does As(III) (e.g., Bowell, 1994; Dixit and Hering, 2003). In reducing environments, As and Sb can be attenuated by adsorbing onto sulfide surfaces or by precipitating as sulfides (Chen et al., 2003; Farquhar et al., 2002; Gallegos et al., 2007; Kirsch et al., 2008; Wolthers et al., 2007).

Although neither As nor Sb are essential to plants, uptake by vegetation and interactions with root processes are also potential controls on As and Sb mobility. Hydrophytes can act as a biological barrier to contaminant movement into the environment, but may also pass contaminants into the food chain and increase mobility through the exudation of organic acids and acidification due to plant processes (Hozhina et al., 2001). Arsenic and Sb concentrations were found to be elevated in the fluvial horsetail (*Equisetum fluviatile*), the same species found in the aqueous environment near the Giant Mine (Brooks et al., 1981; Hozhina et al., 2001).

1.2. Controls on As and Sb speciation

In water, the redox couples (As(III/V)) and (Sb(III/V)) commonly do not reach equilibrium and these species are often found in concentrations that are in excess of what would be predicted thermodynamically (Filella et al., 2002; Inskeep et al., 2002). Discrepancies between thermodynamic predictions and field observations may be attributed to slow reaction kinetics, biological activity, and photo-oxidation processes (Bertine and Lee, 1983; Filella et al., 2002; Krupka and Serne, 2002; McCleskey et al., 2004). Although they are often closely associated and have similar electronic structures, As and Sb exhibit different redox properties whereby the oxidized species of Sb and reduced species of As can coexist in solution (Mitsunobu et al., 2006; Mok and Wai, 1990).

Oxidation of As and Sb by oxygen alone has been shown to be slow, ranging from months to years (Cherry et al., 1979; Eary and Schramke, 1990; Leuz et al., 2006b), but Fe and Mn oxides and humic acids have been shown to catalyze the oxidation of both As and Sb (Belzile et al., 2001; Buschmann and Sigg, 2004; Kneebone et al., 2002, and references therein; Kuehnelt et al., 1997; Leuz et al., 2006a; Manning et al., 2002; Watkins et al., 2006). Reduction of Sb(V) on the surfaces of nanoparticulate magnetite and mackinawite has also been observed (Kirsch et al., 2008). Both As(III) and Sb(III) can be oxidized by microbial processes of chemolithoautotrophy, respiration, and detoxification (Ehrlich, 2002; Fillela et al., 2007; Stolz et al., 2006). Microbially mediated oxidation rates for As(III) are greatly enhanced over inorganic rates (e.g. Nordstrom, 2003). Little is known about microbially mediated Sb(III) oxidation rates but results from Asta et al. (2012) indicate that such rates also are enhanced over inorganic rates but are substantially slower than microbially mediated As(III) oxidation and this is likely to be the same for rates of reduction.

1.3. Study area

Giant is an underground gold mine located 5 km north of Yellowknife, NWT, Canada, on the northern arm of Great Slave Lake (Fig. 1). The mine was active for fifty years, between 1948 and 1999. The mine area includes a roaster and settling and tailings ponds. Baker Creek flows through the mine property (Fig. 2) and has been impacted by tailings spills and decants, discharge from the water treatment plant and possibly historic stack emissions (Jamieson, 2014). Baker Pond (BP) lies on the stream path immediately downstream of the settling pond and polishing ponds associated with the water treatment plant (Fig. 2). From BP, water empties into Baker Creek, which flows through the mine site and discharges into Yellowknife Bay. Two sampling sites, Baker Creek Vegetated (BCV) and Baker Creek Channel (BCC), are located farther downstream at the outlet to Yellowknife Bay (Fig. 2).

1.3.1. Ore geology and processing

The ore deposits are located in the Archean Yellowknife Bay Supergroup greenstone belt, and hosted in deformation and alteration zones that crosscut the Kam Group mafic volcanics (Canam, 2006). The ore zones contain up to 15%, but more often less than 5% sulfide minerals, which include pyrite, arsenopyrite, sphalerite, chalcopyrite, stibnite, Sb-bearing sulphosalts and pyrrhotite (Coleman, 1957). The Au was refractory and hosted primarily in arsenopyrite, and to a lesser extent in pyrite and quartz (Coleman, 1957). To extract gold, processing consisted of four steps: crushing, floatation, roasting, and cyanidation. Roasting was conducted at 500 °C over two stages to oxidize the As and S and convert the arsenopyrite and pyrite into porous iron oxides (maghemite and hematite) amenable to cyanidation. The volatile phase of As was As_2O_3 which was condensed and collected in the baghouse. The Sb gaseous phase was most likely Sb_2O_3 (Marsden and House, 2006; Riveros et al., 2000); the mixed oxidation-state Sb mineral, Sb_2O_4, could also have been thermodynamically stable under the roasting conditions (Asryan et al., 2003), and a vitreous and sparingly soluble $(As,Sb)_2O_3$ phase also was reported (Riveros et al., 2000). Details of ore processing at Giant is covered by More and Pawson (1978), McQuiston and Shoemaker (1975), and Walker et al. (2005, 2015). The same roaster was used from 1958 to 1999 and changes were reportedly minor and would have ensured a consistent calcine (Marsden and House, 2006).

Arsenic and Sb are associated with maghemite and hematite as As(III) and As(V), and Sb(III) and Sb(V) (Fawcett and Jamieson, 2011; Walker et al., 2005). The association of both oxidation states with the roaster oxides suggests that complex solid–gas phase reactions did occur in the roaster and multiple forms of the metalloids were available to associate with the Fe-oxides.

Processing produced three tailings streams: the floatation tailings which consist dominantly of silicate minerals remaining after sulfide removal, the calcine which consists of As and Sb-rich cyanided roaster-derived material, and the Electrostatic Precipitator (ESP) residue consisting of the cyanided particulate material in the roaster discharge gas. The calcine is composed of fine grains, 90% < 0.045 mm, and the ESP is composed of very fine grains, 90% < 0.014 mm. The floatation tailings comprised the largest volume waste stream but had the lowest As and Sb concentrations, whereas the calcine and ESP dust comprised the smallest volume but contained the greatest concentrations of As and Sb (Fawcett et al., 2006; Walker et al., 2015). The dominant minerals in the

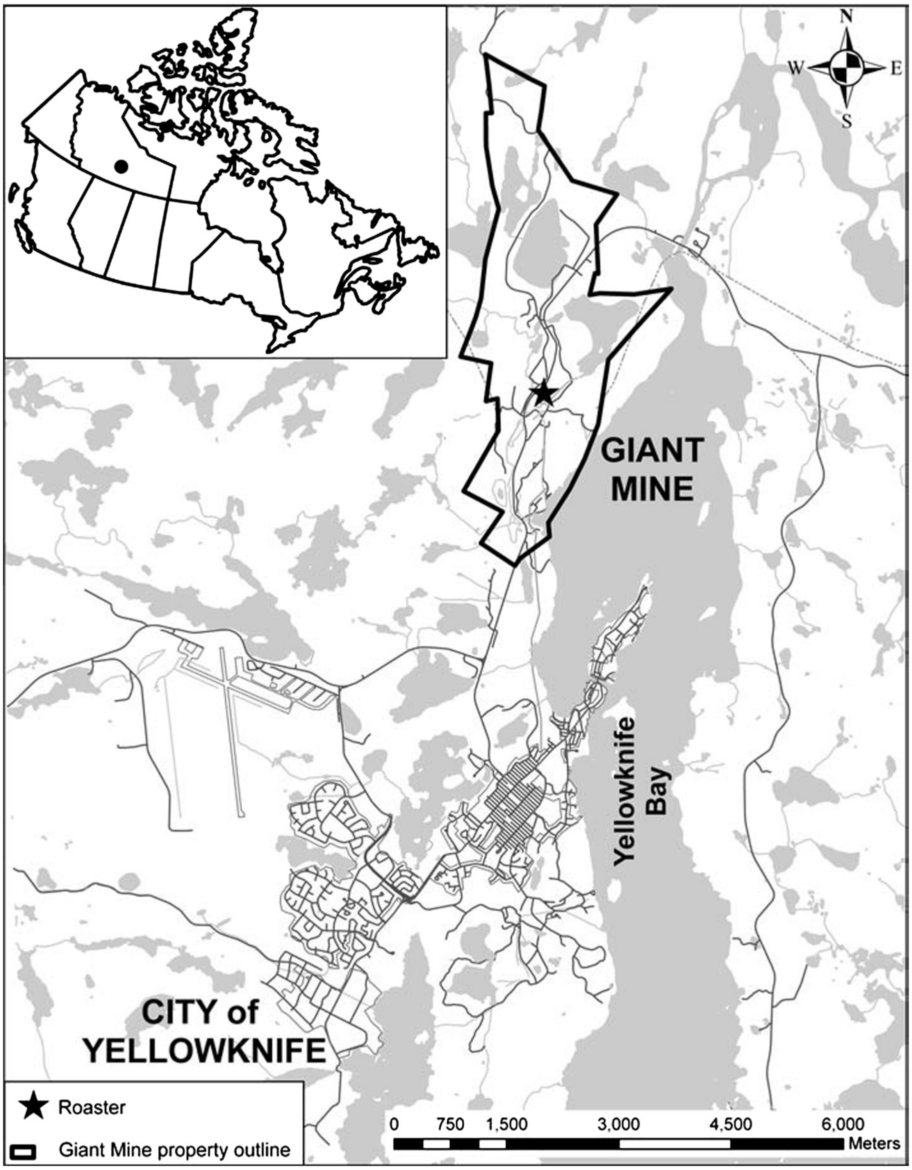

Fig. 1. Location map, Giant Mine, NWT, Canada.

tailings are quartz, dolomite, chlorite, muscovite and calcite (Walker et al., 2015). Acid mine drainage does not occur since sulfide content is low relative to carbonate.

1.3.2. Water treatment and sediment deposition

The water treatment system began operation in 1981 and was in operation during this research project. Because of the freezing conditions throughout most of the year, the water treatment plant is only operational during the summer months. At the time of writing, the system is treating water pumped from the underground mine workings, and held in NorthWest Pond and in North Pond during high flow events. The water treatment system involves the addition of H_2O_2 to oxidize the As, ferric sulfate to promote the precipitation of arsenates, and a flocculating agent and lime to remove As and other mining-related metals (i.e. Pb, Zn, Cu). The sludge and treated water is discharged to the settling pond, and eventually flows to the polishing pond.

Prior to the construction of the water treatment plant, only the uppermost tailings area was used during the winter, and slurries accumulated over the 7–8 month winter. Ice accumulated in all three tailings areas, sometimes to levels higher than the dams. Consequently, spring melt, which happened first in the upper tailings pond, resulted in a large amount of tailings slurry (composed of the fine fraction waste streams) being transported over the ice and breaching the dams. Significant quantities of solids escaped the third (final) tailings area during turbulent spring flow events (Berube et al., 1974). Since Baker Pond was probably impacted by these spring overflow events, the sediment chemistry should reflect these events of significant tailings deposition.

A breakwater at the outlet to Yellowknife Bay was constructed in 1964, which altered depositional patterns: sediment was preferentially deposited in the area of BCV, and a channel along the breakwater resulted (Fig. 2). Air photo studies show that the outlet to Yellowknife Bay did not become vegetated, nor was subject to substantial sedimentation, until 1966–1970. The BCC and BCV sites would have been impacted by the same turbulent spring flow events that affected BP. Baker Creek was also impacted by numerous tailings spills originating from faulty tailings pipelines (Giant Yellowknife Mines Limited, 1981). As can be seen in Fig. 1, BCV is now densely vegetated. The primary plant population is the annual aquatic horsetail (*E. fluviatile*).

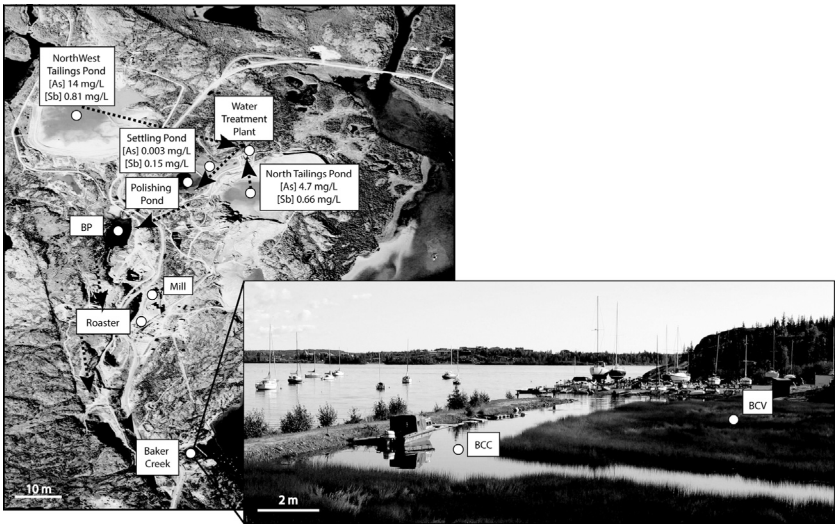

Fig. 2. Site locations at Giant Mine and As and Sb concentrations in the tailings and water treatment ponds, samples collected September, 2005. Water flow is along the path of the black arrows.

2. Methods

2.1. Sample collection

Calcine and ESP residue samples were collected from the mill by staff at Giant in 1999 as described in Walker et al. (2005). The samples were dried under nitrogen gas to prevent oxidation and stored in a freezer.

Surface water samples were collected from NorthWest and North tailings ponds, and treated water from the settling pond in September 2005 and July 2006. Surface waters were filtered in the field using 0.22 μm Nalgene filters into HDPE bottles. Dark bottles were used for Fe(II) and total Fe determination and metalloid speciation to avoid photo-oxidation. Water samples collected for cation analysis were preserved with 1% HNO_3, samples collected for speciation and Fe(total) and Fe(II) determinations were preserved with 1% HCl (McCleskey et al., 2004). All acids used were trace-metal clean grade.

Pore-water samples were collected in August 2005 from BP and July 2006 from BCC and BCV. Pore-waters were collected immediately using in-situ dialysis arrays (peepers) (Andrade et al., 2010; Martin and Pedersen, 2002). Prior to peeper deployment, the equipment was cleaned with Sparkleen™, rinsed with distilled de-ionized water (DDW), soaked in ultrapure nitric acid, and again rinsed with DDW. The peepers were assembled with DDW in the cells and placed in DDW-filled cases. The cases were submerged in aquariums heated to 37 °C to enhance diffusion of oxygen from the cells, and bubbled with ultrapure nitrogen daily for two weeks. Two peepers were deployed at each site by approaching the site from downstream (BP-from a dock) to ensure minimal disturbance. They were pushed into the sediment −22 cm to −44 cm (depending on substrate), and the numbers of cells above the interface were recorded. Equilibration time was two weeks. Prior to peeper extraction the cases were purged with N_2 and covered to avoid the occurrence of any redox reactions in transit.

Sediment cores were collected immediately adjacent to the peepers using a gravity corer (Glew, 1989) and transparent polycarbonate core tubes 60 cm in length and 7.5 cm in diameter. One sediment core was collected from BP in August 2005, and from BCV and BCC in July 2006. Two horsetail plants with fully submerged roots were collected in July 2007 from the Baker Creek Vegetated (BCV) site, washed and chilled.

2.2. Sample preparation

Cell water extraction was undertaken in a laboratory in a glove bag purged with N_2. The cleaned membrane is pierced with a trace metal free pipette tip, cell water is extracted using a pipetter (approximately 6 mL can be extracted from each cell), and placed in N_2 purged HDPE containers (dark containers for the redox-sensitive species analysis) (Andrade et al., 2010; Martin and Pedersen, 2002). New pipette tips are used after every cell to avoid cross-contamination. Samples were immediately preserved and chilled. The pH was measured immediately after extraction. It was not possible to measure Eh or DO due to the small sample volume, so Fe(II) and SO_4 were used as proxies for the redox status of the pore waters, as explained below.

Sediment cores were immediately covered following collection to avoid photo-oxidation reactions during transport and were extracted in the laboratory, in a N_2-purged glovebag, at 0.5 cm, 1 cm, or 2 cm intervals. The extruded core samples were immediately frozen for transport. Sediment samples to be analyzed for bulk chemistry were freeze-dried and samples for X-ray Absorption Near Edge Structure (XANES) analyses were dried under a N_2 atmosphere. Ten BP core sub-samples and 8 BCV core sub-samples were selected for XANES analyses based on their depth distribution. XANES samples were mounted in 3 mm-thick Teflon holders and sealed with Kapton™ tape.

2.3. Analyses

Concentrations of major cations and trace metals in aqueous samples were determined using inductively-coupled plasma-atomic emission spectrometry (ICP-AES) (Leeman Labs – DRE). Total dissolved As and As(III) and total dissolved Sb and Sb(III) were determined by hydride generation atomic-absorption spectrometry (HG-AAS) using a method similar to that of McCleskey et al. (2001). Concentrations of total dissolved Fe and Fe(II) were determined using a modification of the FerroZine colorimetric method (Stookey, 1970; To et al., 1999) with a UV–VIS spectrophotometer (HP 8453). Concentrations of major anions were determined by ion chromatography (Dionex 600) (Brinton et al., 1995). Alkalinity (as HCO_3^-) was determined by auto-titration (Orion 960/940) using standardized H_2SO_4 (Barringer and Johnsson, 1989). All reagents were of purity at least equal to the

Table 1
Relative Standard Deviation (RSD) calculations of sediment standards and sediment sample duplicates.

Standards	Sample population	RSD (%)	
		As	Sb
G1	3	0.1	0.1
DS7	2	1.2	3.3
DS6	2	3.6	2
Duplicates[a]	10 sets	2.8	2.9

[a] RSD reported for duplicates is the average of 10 sets, RSD's of As range from 0 to 11.7, Sb from 0 to 9.19.

reagent-grade standards of the American Chemical Society. Double-distilled water and re-distilled acids were used in all preparations. U.S. Geological Survey standard reference water samples (SRWS) were analyzed as unknowns along with the samples to check for accuracy. The SRWSs AMW4, T163, T179, T181, M150, M156, M158, and M172 were used to check the analytical methods for the As, Sb, Fe, and SO_4 determinations (Farrar, 2000; Connor et al., 2001). The SRWSs were analyzed several times during each analytical run. The percent differences between the measured value and the reported most probable value (MPV) was 99–101% for As, 97–104% for Sb, 95–105% for Fe, and 100–104% for SO_4.

Pore-water samples collected from BCC and BCV were analyzed for S(-II), Fe(II), and SO_4 using the Hach DR/2400 portable spectrophotometer. The parameters were analyzed in the order listed to minimize artifacts from sample oxidation. A detailed account of using the Hach spectrophotometer on smaller volume samples is provided by Craigen (2006).

Elemental analysis was carried out on 73 sediment core subsamples from BP, BCC, and BCV using hot aqua regia digestion and subsequent analysis by ICP-MS at ACME Analytical Laboratories, Vancouver, Canada. The QA/QC calculations for laboratory standards and duplicates are shown in Table 1.

Previous work (Walker et al., 2005) on samples from Giant Mine has shown that conventional X-ray diffraction is rarely useful for identification of As- and Sb-bearing phases because they are present in low modal quantities. Synchrotron-based microXRD has the advantage of grain-specific analysis and the effective filtering of quartz, feldspar and other silicates that would dominate a conventional XRD pattern, which are eliminated from the diffraction pattern because they are too coarse-grained to diffract under most synchrotron microprobe experimental conditions (Jamieson et al., 2011).

The XANES spectra of BP, and BCV sediment, the calcine, and the ESP residue were collected at the Sb K-edge (30,491 eV), and six sediment samples from BP, the calcine and ESP residue at the As K-edge (11,868 eV), over two sessions at the PNC-XOR undulator beamline 20-ID at the Advanced Photon Source. Because the BCV samples contained a significant amount of organic matter, a thermoelectric cryostage was used to cool the samples to −20 °C to avoid beam-induced oxidation or reduction of Sb due to the burning of organic matter. A Si(3 1 1) double-crystal monochromator was used to control the X-ray energy and spectra were collected in fluorescence mode using a 7-element Canberra Ge(Li) detector. Three to five scans were collected for each sample. Individual scans were calibrated to an Sb_2O_3 standard run simultaneously. The first and last scans exhibited consistent edge position, thereby confirming no beam damage had occurred. The beam size used in the collection of bulk XANES data was 0.5 mm.

Processing of XANES data was carried out using ATHENA software. Linear combination fitting was performed on the normalized As spectra, 50 eV over the edge position, and on the Sb derivative spectra 100 eV over edge position (Fawcett et al., 2010). The model compounds used in fitting Sb K-edge spectra were selected based on findings in Fawcett et al. (2010) and include Sb_2O_5 and Sb_2O_3 obtained from Fisher Scientific, and tetrahedrite from the Miller Museum at Queen's University (M361). Scorodite, arsenolite, arsenopyrite, and orpiment were employed in fitting As K-edge spectra. Scorodite (M6303) and arsenopyrite (M5579) were acquired from the Miller museum at Queen's University, arsenolite is a J.T. Baker reagent, and orpiment was acquired from the APS standards collection.

Synchrotron-based element maps were collected during the same sessions as the XANES collection by orienting thin sections 45° to the beam and scanning with a reduced beam size (5 μm compared to 0.5 mm used for bulk XANES analyses). The setup and capabilities of the microprobe end station at PNC/XOR are described in detail by Heald et al. (2007). Environmental Scanning Electron Microscopy (ESEM) was performed on the Zeiss Evo 50 Environmental Scanning Electron Microscope at the Geological Survey of Canada in Ottawa on the two BCV thin sections that were mapped by synchrotron microprobe. The ESEM utilizes an Oxford Inca Energy 450 X-ray micro-analysis system for elemental and phase analysis.

The horsetail samples were analyzed for total elemental concentrations by ICP-AES at the Analytical Services Unit, Queen's University, Canada. Based on duplicate samples, the relative standard deviation of As in plant analyses is 6.5%, and Sb is 3.4%.

3. Results

3.1. Roaster products

The total concentrations of As and Sb were high in the calcine and ESP residue relative to sediments at the study site: 3317 ppm Sb and 24,905 ppm As in the calcine, and 10,677 ppm Sb and 40,460 ppm As in the ESP residue (Fig. 3). Roasting produced multiple As and Sb phases: As(V) bound to oxygen (As(V)–O) and As(III) bound to oxygen (As(III)–O). Residual arsenopyrite (As(-I)–S) is also present. Antimony is present as only two phases: Sb(V) bound to oxygen (Sb(V)–O) and Sb(III) bound to oxygen (Sb(III)–O). In the XANES region, only the oxidation state and the next-nearest atom can be determined (based on shape and edge-position comparisons with model compounds), but not the specific compounds. Additionally, it is not possible to distinguish between a mixed-oxidation state mineral and a sample containing a combination of mineral phases (Fawcett et al., 2010). The Sb(V):Sb(III) ratio was 1.5 in the calcine and 0.41 in the ESP dust, suggesting that the mixed phase $Sb(III)Sb(V)O_4$, with a ratio of 1, is not present or only in trace amounts.

Although it is evident that most of the arsenopyrite was oxidized in the roaster, some did remain in the calcine. However, none of the Sb-sulfide minerals originally present in the ore remained in the roasted material. The As and Sb oxide phases showed a similar pattern in that there is a higher proportion of As(V)–O and Sb(V)–O phases in the calcine, and a higher proportion of As(III)–O and Sb(III)–O phases in the ESP residue (Fig. 3).

Table 2
As and Sb concentrations in tailings and water treatment ponds, samples collected in September 2005 and July 10 2006. All values in mg/L.

Water samples	2005		2006	
	As	Sb	As	Sb
NorthWest Pond	13.9	0.813	26.8	1.62
North Pond	4.73	0.655	2.64	0.926
Settling Pond	0.003	0.146	0.001	0.165

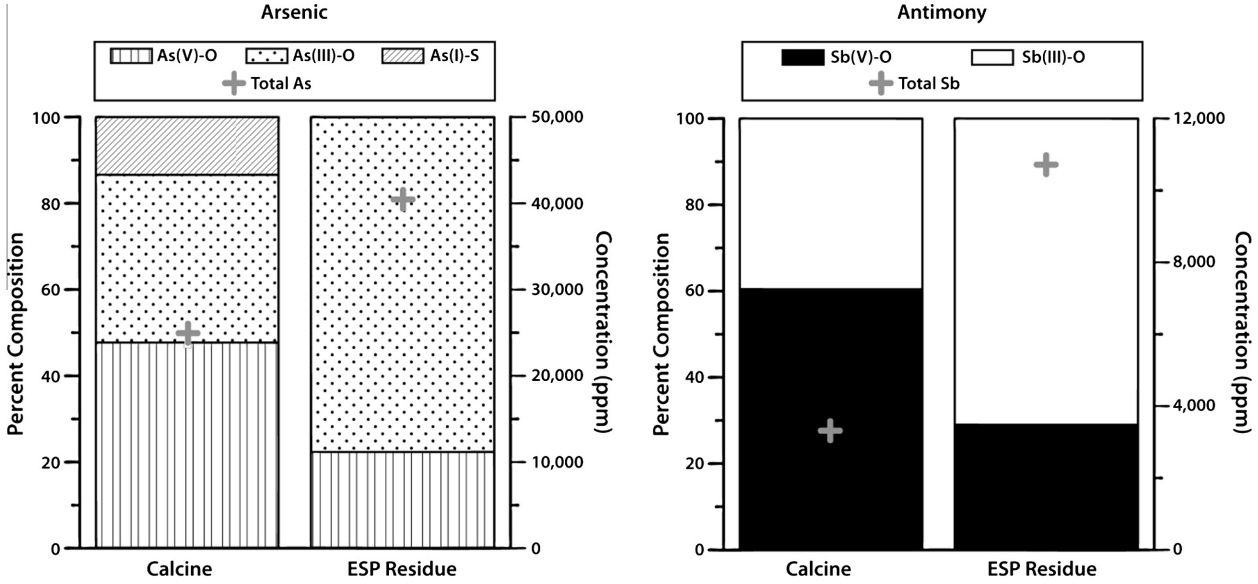

Fig. 3. Arsenic and antimony concentrations and linear combination fits of XANES spectra of calcine and ESP residue.

3.2. Water from tailings ponds

The pH in the tailings, settling, and polishing ponds ranged from 7.4 to 8.31. Concentrations of As and Sb in the tailings ponds were elevated (Fig. 2, Table 2) relative to the Canadian drinking water guidelines (0.010 and 0.006 mg/L, respectively) and relative to the mine effluent guidelines of 0.5 mg/L, reflecting the elevated concentrations of As and Sb in the mine water pumped from the underground workings into the tailings ponds. In all samples of tailings pond water, As(III) and Sb(III) comprised less than 3% of the total As and Sb. Concentrations of As and Sb differed between the two tailings ponds, as well as by year (2005 and 2006), likely reflecting variations in host rock in the underground locations from which the water was pumped.

The most significant finding from the surface water data is that Sb remained elevated in water after treatment. Arsenic, on the other hand, was effectively removed by the water treatment system to below the effluent discharge limit of 0.5 mg/L, and even below drinking water guidelines. These results are consistent with the findings of Milham and Craw (2009) and Nishimura and Umetsu (2000).

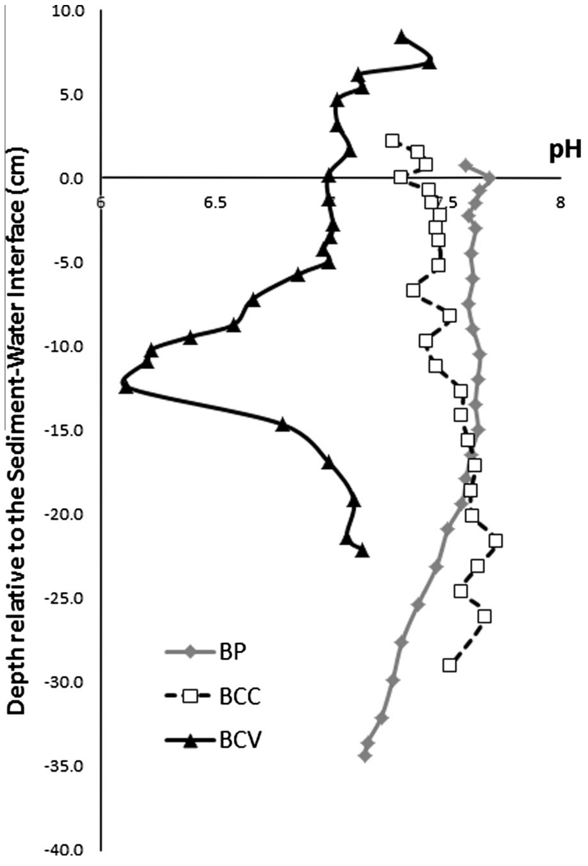

Fig. 4. Pore-water pH profiles for BP, BCV, and BCC.

3.3. Sediment and pore-water

3.3.1. Substrate

The Baker Pond sampling site (BP) comprised very fine-grained sediment that occupies the northernmost section of Baker Pond. The water at the time of sampling (August 2005) was approximately 1.5 m above the sediment–water interface (SWI). The 32 cm long core (7.5 cm diameter) was massive in appearance and light gray in color. Very little vegetation grows on this substrate that has been undisturbed for approximately 25 years. The BCV core showed three distinct zones. The top 10 cm was composed primarily of vegetation and organic material. The middle zone (5.5 cm) was a mixture of inorganic sediment and organic material, and the deepest zone was a light gray and orange clay material. The BCC core was brownish colored in the top 8 cm and gray in the deeper parts. The top of the core is a mixture of clay and coarser grains, which gradationally changes with depth to clay-rich sediment. The channel sediment is unvegetated.

3.3.2. Total concentrations in sediment and pore-water

As shown in Fig. 4, pH values in pore-water are close to neutral. Concentrations of Fe, Ca, S, and Mn in sediment are shown in Fig. 5. Elevated As and Sb concentrations throughout the entire length of the core from BP indicate that sediments down to −35 cm have been impacted by mining activities (Fig. 6). The Canadian interim sediment quality guideline for As is 5.9 ppm. There are no Canadian sediment quality guidelines for Sb. In the sediment, the

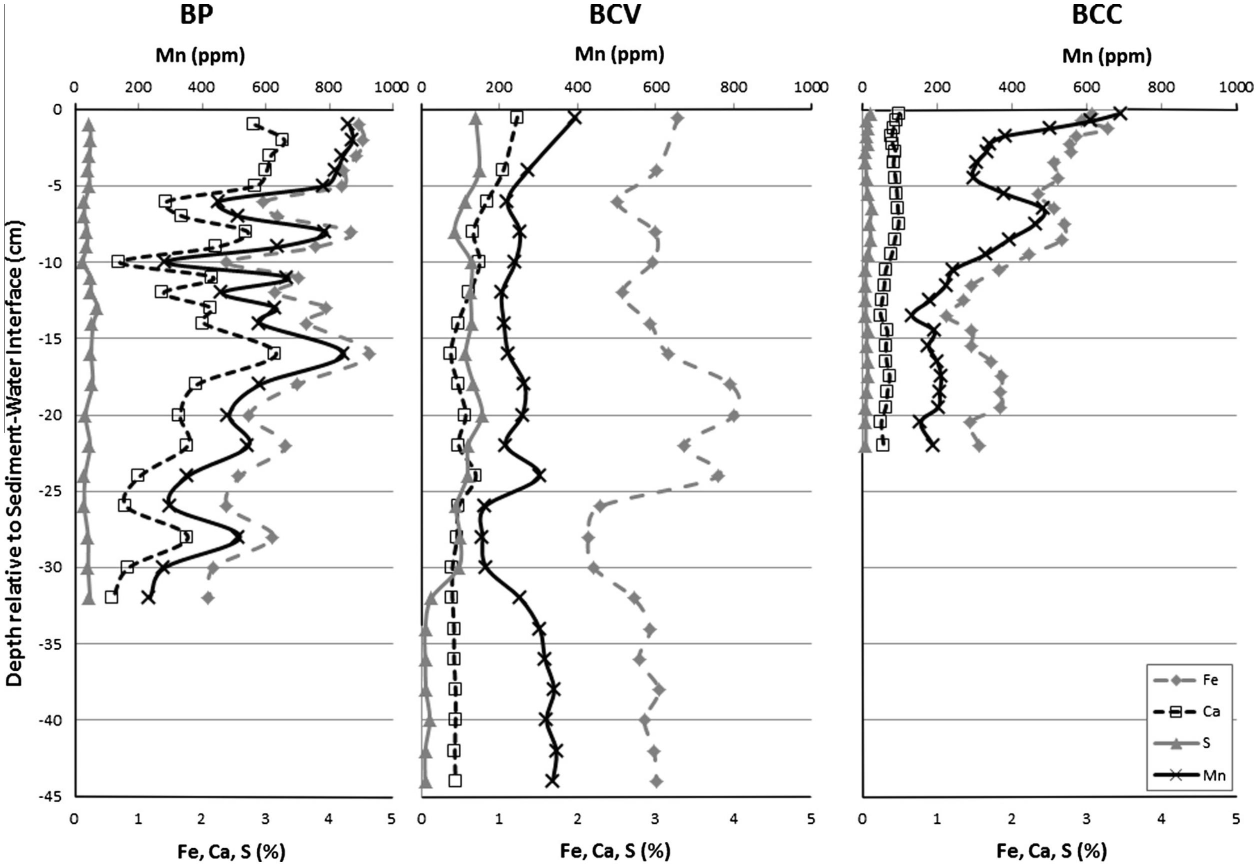

Fig. 5. Distribution of Fe, Ca, S and Mn in BP, BCV, and BCC sediment.

maximum concentrations of As were 2000 ppm and of Sb were 461 ppm, and in the pore-water, maximum concentrations were 62.3 mg/L and 1.97 mg/L, respectively. The concentrations of As and Sb in pore-water at BP were much higher than those at BCC and BCV. Although the distribution of As and Sb in sediment at BP was similar, their distribution in the accompanying porewater samples was dissimilar. Aqueous Sb was highest between 0 and −2.5 cm (surficial layer), higher than in the surface water immediately above the sediment–water interface (0.32 mg/L), indicating the sediment is a source of aqueous Sb. In contrast, As was concentrated between −7.5 cm and −22.5 cm. The normalization ratios of aqueous concentration/sediment concentration (representing the mass of element released to the pore-water per mass of element in the sediment) generally were higher for As than for Sb, indicating that As was more readily mobilized than Sb, except in the surficial layer where the ratio for Sb was higher than that for As.

At BCV, the maximum concentrations of As and Sb in sediment were 3670 ppm and 1069 ppm, respectively; the highest sediment concentrations of the three sites studied. Distributions of As and Sb were similar in sediment and in pore-water except between −4 cm and −8 cm where As appeared to have partitioned preferentially into the pore-water, and the normalization water/sediment ratio indicated an increase in mobilization of As over the same interval. Between −10 cm and −15 cm, aqueous As and Sb concentrations increased and pH decreased to 6.1 from a maximum of 7.4 above and below the interval, coinciding with a peak in S^{2-} concentration to 44 μg/L from 35 μg/L above and below the interval. Overall, As and Sb at this site appear to be well attenuated given that the normalization ratio plotted in Fig. 6c is two orders of magnitude lower than those shown for BP and BCC.

The maximum concentrations of As and Sb in sediment were lower at BCC than at the other sites, 580 ppm and 63 ppm, respectively. As observed in BP and BCV, the distribution of As and Sb in BCC sediment was similar yet the distribution of aqueous As and Sb was different. Antimony was elevated in the pore-water only at and above the sediment–water interface (SWI). Aqueous As, but not Sb, was elevated over the mid-core enrichment interval. Overall, the normalized profile indicates As to be more readily mobilized than Sb.

3.3.3. Aqueous speciation

It is widely recognized that disequilibrium conditions dominate with respect to redox reactions in low-temperature aqueous systems (Nordstrom and Munoz, 1994; Langmuir, 1997; Sigg, 2000; Appelo and Postma, 2005; Nordstrom and Campbell, 2013) and that rates are often microbiologically catalyzed and determined by microbial growth kinetics (Banfield and Nealson, 1997; Ehrlich, 2002). Hence, the approach taken in this study was to characterize the redox conditions in these waters by measuring the concentrations and trends of the main redox species (Fe, S, As, and Sb).

At BP, As(V) was the predominant species in pore-waters from 0 to −2 cm, below which As(III) dominates (Fig. 7a). In contrast, Sb(V) persisted as the more prevalent Sb species at all depths (Fig. 7b). At BCV, most of the sediment profile below the SWI appears to be more reducing than the sediments at BP, as indicated by the relatively high Fe(II) concentrations (20–22 mg/L over the interval from −5 cm to −20 cm) and lower SO_4 concentrations (3–6 mg/L over the same interval) (Fig. 7c). With the exception of one sub-sample above the SWI, the most prevalent As species is As(III). As was seen in BP, Sb(V) is the dominant Sb species at BCV. At BCC, Fe(II) and SO_4 concentrations indicate an oxidized zone from 0 to −12 cm and more reduced conditions deeper in the profile. Arsenic speciation in the pore-waters at BCC was variable. Sb(V) was the dominant Sb species present, as seen in BP and BPV pore waters.

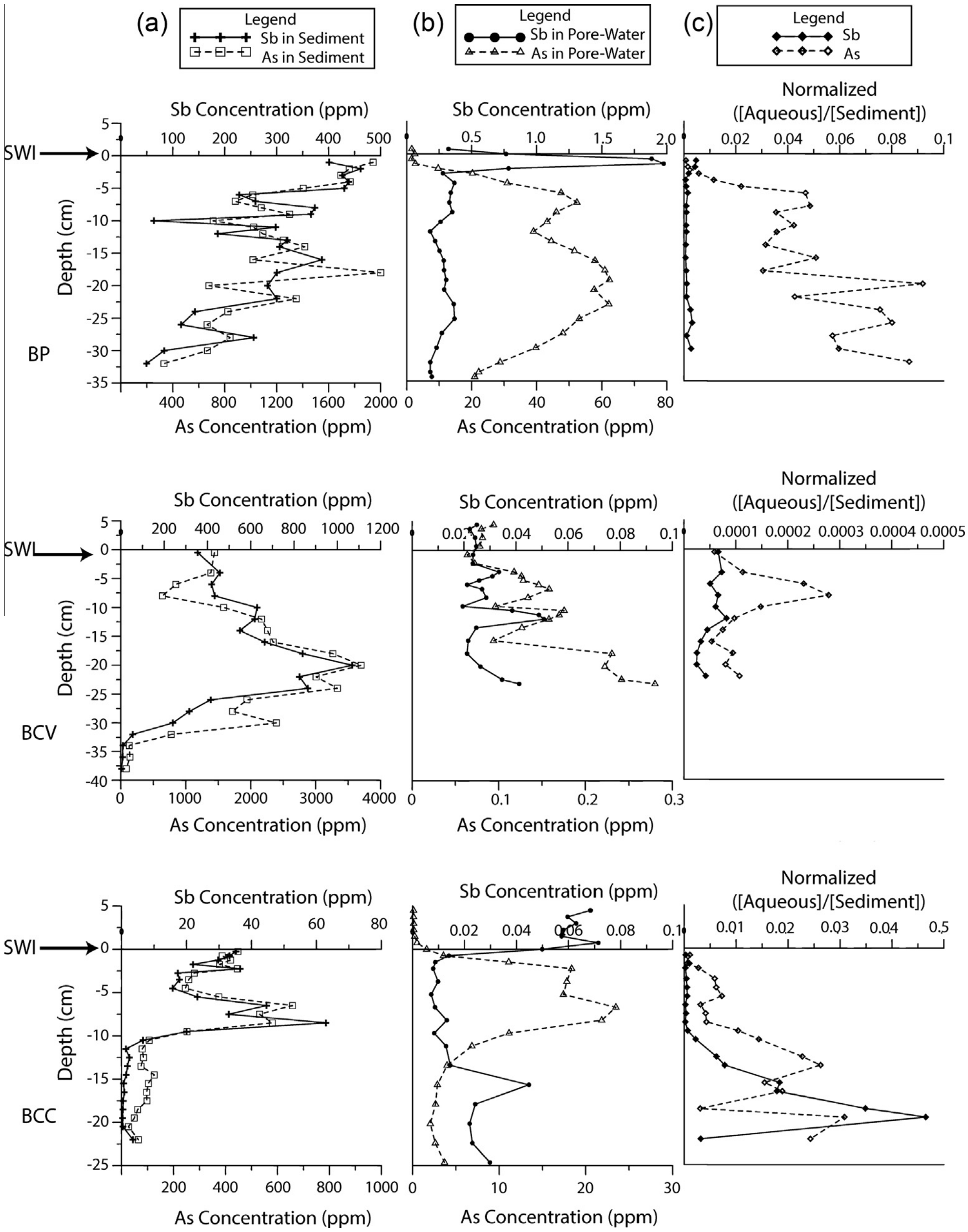

Fig. 6. Distribution of As and Sb in sediment and pore-water (a) distribution of As and Sb in sediment with depth, (b) distribution of As and Sb in pore-water, (c) the normalized value indicates the ratio of aqueous concentration to sediment concentration and is an indicator of the degree of mobilization. SWI = sediment–water interface.

3.3.4. Solid-state speciation

In the sediment core from BP, the relative percentage of As(V)–O decreases with depth and an As(III)–S phase appears at −16 cm (Fig. 8a). Arsenopyrite (As(-I)–S) is present at all depths in approximately the same percent composition (12–17%). The As(III)–O phase is also present in all samples. Similarly, the Sb(III)–O phase is present in all samples (Fig. 8b) and an Sb(III)–S phase appears at −12 cm and represents an increasing proportion of the sample with depth. However, the percentage of the Sb(V)–O phase does not decrease with depth, as observed for the As(V)–O phase, but persists as the most dominant phase at all depths. In the BCV samples, the persistence of the Sb(V)–O phase and an Sb(III)–S phase deeper in the core (Fig. 9) is similar to the solid-state speciation profiles for BP. The Sb(III)–S phase was first detected at −6 cm, was not present in the −10 cm sample, was detected again at −16 cm and subsequently increased with depth. Arsenic XANES was not done on BCV samples.

3.4. Aquatic vegetation

The two aquatic horsetail samples, BCVP-1 and BCVP-2, contained 1031 ppm and 1789 ppm As, and 123 ppm and 146 ppm Sb, respectively. Within 0 to −10 cm (the interval containing the greatest amount of vegetation) As concentrations in the sediment ranged from 641 ppm to 1441 ppm, and Sb concentrations ranged from 354 ppm to 433 ppm. The association of both elements with vegetation in the surficial zone is confirmed with microprobe mapping and ESEM images shown in Fig. 10. Aggregates produced by thin section preparation are dominated by with organic material (fragments of vegetation or inorganic material such as mineral grains). Although the As and Sb elements maps look slightly different due to different synchrotron beam penetration during mapping, the aggregates are recognizable and can be matched with those in the ESEM-BSE image. Aggregates are labeled O for organic or I for inorganic based on visual inspection and the intensity of the carbon signal in the ESEM spectra

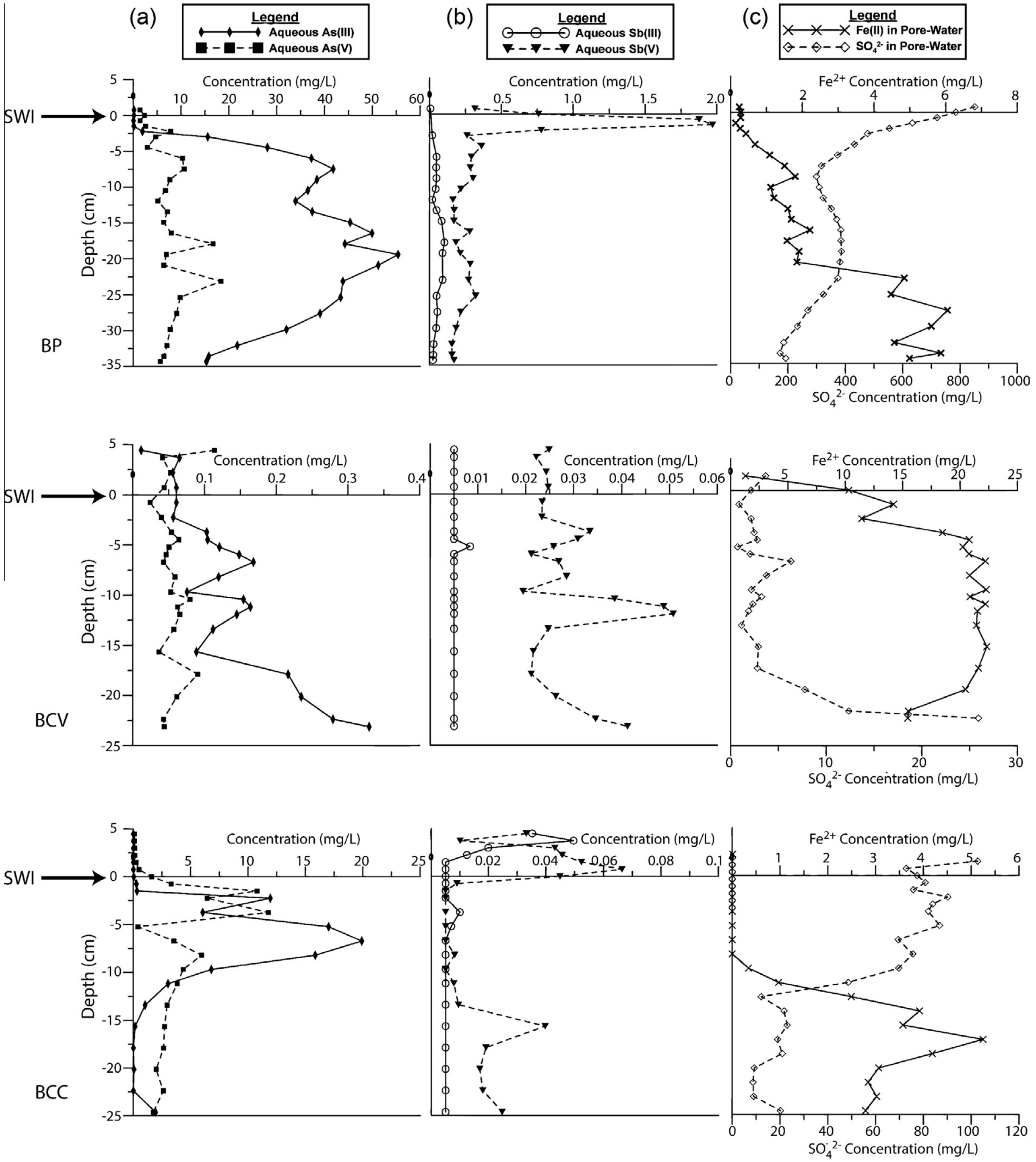

Fig. 7. Aqueous speciation of As, Sb, Fe, and SO_4 in BP, BCV, and BCC, SWI = sediment water interface (a) aqueous As species, (b) aqueous Sb species, in BCV and BCC some Sb(III) data is plotted at the detection limit of 0.005 mg/L, (c) Fe(II) and SO_4^{2-} concentrations. SWI = sediment–water interface.

(not shown). Fig. 10a–c shows the ESEM-BSE (backscattered electron) image and microprobe maps of the thin-section prepared using sample from BCV-1, the sample collected 1 cm above and below the defined sediment–water interface. Although there are some small high-count spots in the inorganic aggregates, as seen in the microprobe maps, the bulk of the As and Sb is associated with the organic material. Fig. 10b–d shows the ESEM-BSE image and microprobe maps of BCV-10, the sample collected from −21 cm to −23 cm, well below the interval of dense vegetation and root penetration. Although live plant parts are absent from this depth there remains older, buried fragments of plants. At this depth the microprobe maps show an association of As and Sb with the inorganic material, rather than the organic material as was observed in BCV-1.

4. Discussion

4.1. Distinguishing anthropogenic and diagenetic controls on speciation

The solid-state speciation results show a higher proportion of the As(III)–O and Sb(III)–O phases resides in the ESP residue compared to the calcine. Gaseous As_2O_3 was generated in the roaster

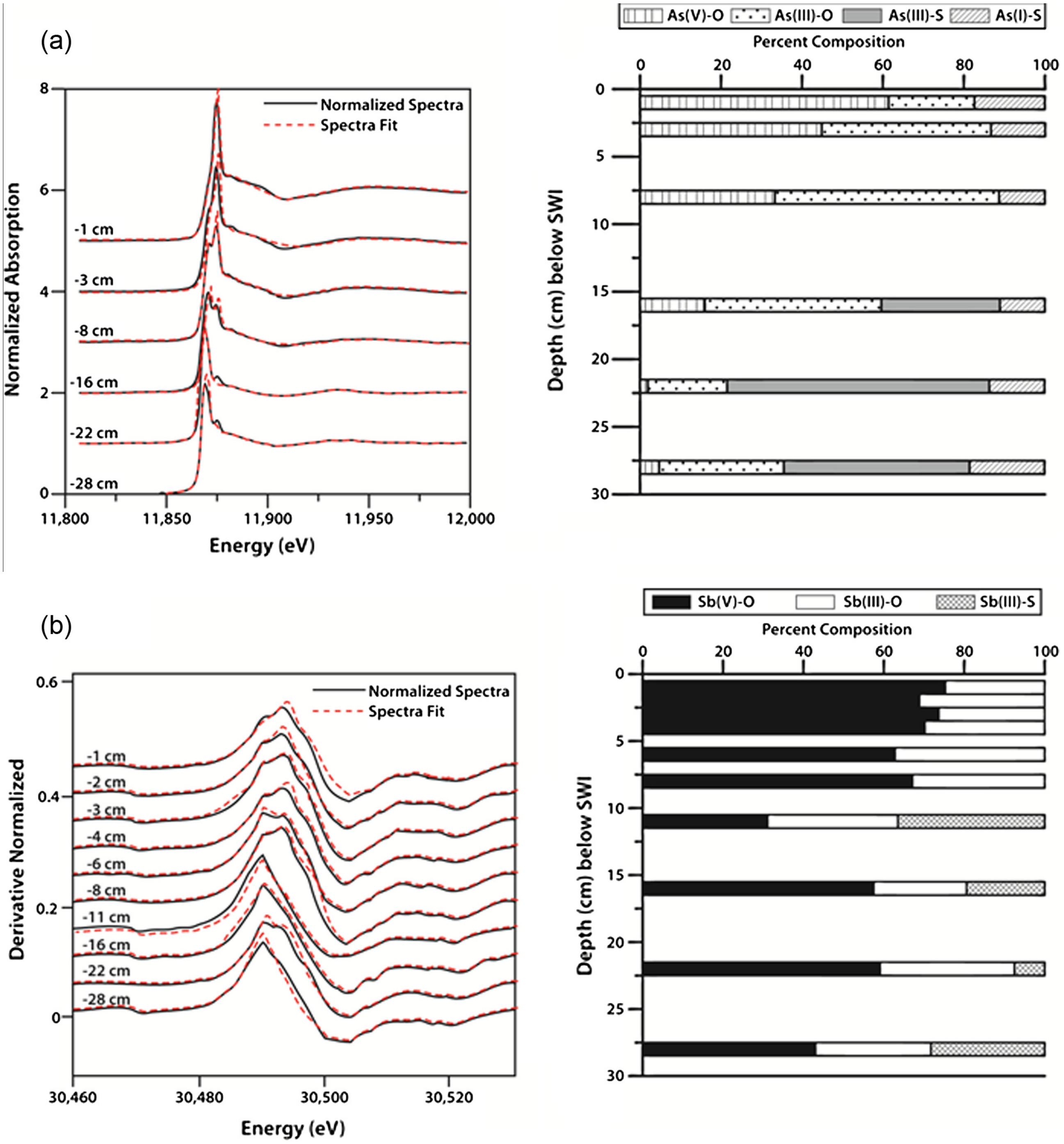

Fig. 8. (a) As and (b) Sb XANES spectra and linear combination fits for Baker Pond (BP) Sediment.

and subsequently sublimated as As_2O_3(s), and reacted with maghemite and hematite as documented by Walker et al. (2005). Arsenic trioxide from stack emissions has persisted in soils near the roaster and rare particles of As_2O_3 have been found in sediments from Baker Creek outlet area (Jamieson, 2014). A volatile Sb phase, likely Sb_2O_3, was also present in the roaster (Riveros et al., 2000). Gaseous phases flowed from the roaster through the electrostatic precipitator before final collection in the baghouse. Based on the flow path, it is reasonable that a greater proportion of the As_2O_3 and Sb_2O_3 ended up in the ESP residue waste stream rather than in the calcine. Also, the Fe-oxide particles feeding into the electrostatic precipitator would have longer interaction times with the volatile phases, and thus the Fe-oxide hosts in the ESP residue waste stream would therefore have higher As(III)–O and Sb (III)–O signatures relative to roaster-oxide grains in the calcine (Fawcett and Jamieson, 2011).

Changes in ore character and processing over time are likely to have only a minor influence on solid state speciation. Mixing of the waste streams was consistent (similar proportions of calcine and ESP residue), as shown by the consistent proportion of arsenopyrite (As(-I)) which was only present in the calcine, but not the ESP residue. Because the speciation of As and Sb coming from the roaster was consistent, any changes in the vertical distribution of affected sediments downstream from the roaster can be interpreted as the result of post-depositional processes. Post-depositional changes in speciation is also evident by the presence

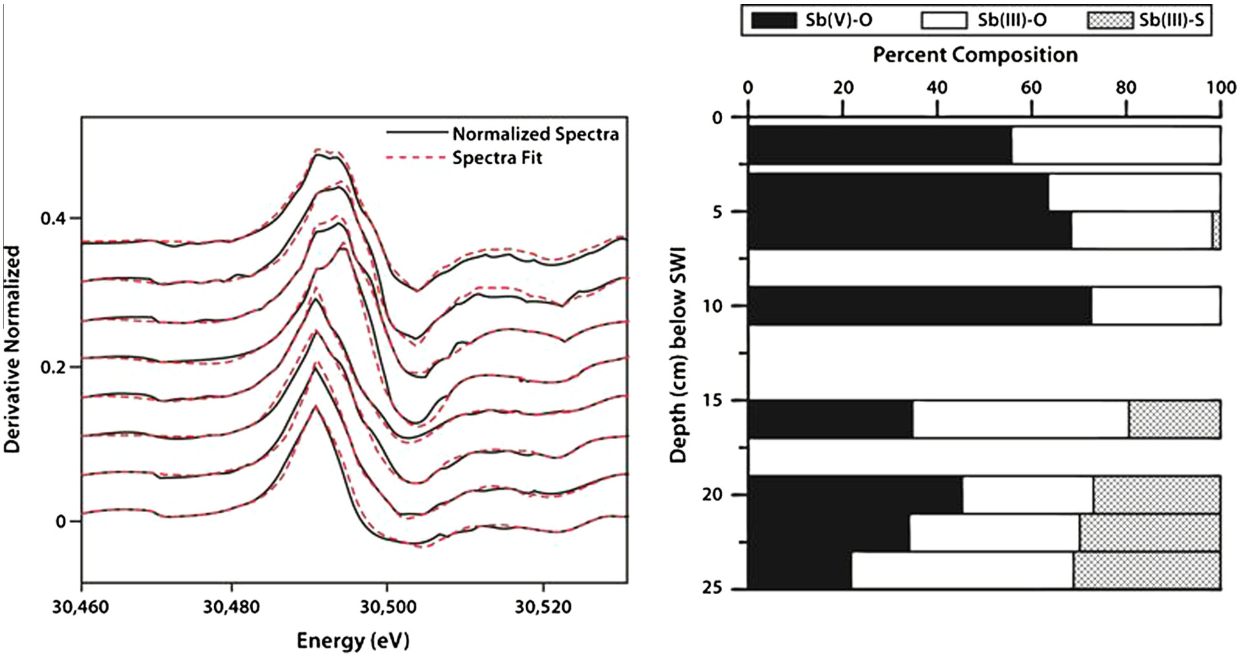

Fig. 9. Sb XANES spectra and linear combination fits for Baker Creek Vegetated (BCV) sediment.

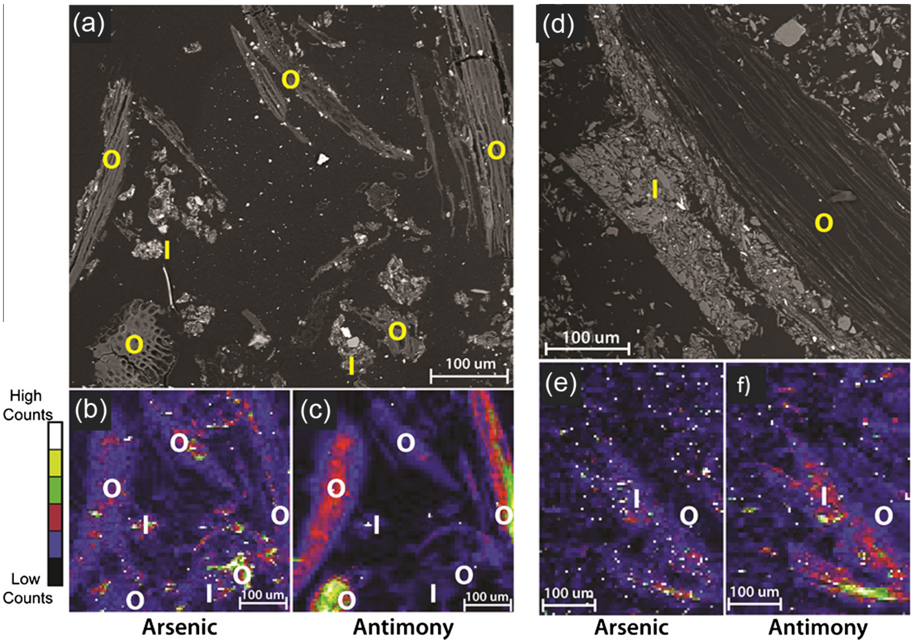

Fig. 10. (a) ESEM-BSE image and synchrotron microXRF maps of (b) As and (c) Sb associated with vegetation from 0 to −5 cm below the SWI (BCV-1), and (d) ESEM-BSE map and synchrotron microXRF maps of (e) As and (f) Sb associated with vegetation from −21 to −23 cm below the SWI (BCV-10). O = Organic material, I = Inorganic mineral grains, confirmed by ESEM and visual inspection.

of the Sb(III)–S and As(III)–S phases in sediment, which are not present in the calcine or ESP residue.

4.2. Controls on mobility

The source of the As and Sb in BP sediment is primarily tailings consisting of the calcine and ESP residue deposited during turbulent spring flow events prior to 1981 (when the mine gained greater control over waste disposal). Fig. 6 shows that in the surficial zone in sediments at BP, Sb concentrations in pore-water are elevated relative to the other sites, indicating a soluble source of Sb. It is unlikely that mobile Sb is due to oxidation of Sb sulfides and sulfosalts in the oxidized zone because the primary Sb minerals were completely converted to oxides in the roaster.

Arsenic attenuation is effective in the surficial, oxidized sediment layers at BP and BCC (an oxidized sediment layer is absent from BCV). In contrast, aqueous Sb concentrations are elevated in the surficial sediment layer at BP, which may be attributed to a number of factors including different mineral solubility controls, different affinities for sorption sites (Ashley et al., 2003; Casiot et al., 2007; Leuz et al., 2006a; Milham and Craw, 2009; Mok and Wai, 1990), or competition for sorption sites, where

As(V) out-competes Sb(V) for sorption sites in the oxidized near-surface.

Below the surficial sediment layers where low-oxygen conditions prevailed at BP, BCC, and BCV, the reduced species of As and the oxidized species of Sb dominated. Most notably at BP and BCC, the distributions of pore-water As and Sb below the surficial layer also differed. Their different behavior, the attenuation of Sb and increased mobility of As, may be explained by their different adsorption dynamics. With progressively more reducing conditions with depth, As(V) adsorbed onto the Fe and Mn oxides likely would be reduced to As(III). Because As(III) does not sorb as strongly as As(V) (Pierce and Moore, 1982; Bowell, 1994), As should partition into the aqueous phase as As(III). This supposition is supported by the solid-phase speciation data where the abundances of the As(V)–O phase were negatively correlated with depth, indicating that this phase was becoming depleted as redox conditions became more reducing with depth. Furthermore, as the As(V)–O was depleted in the sediment, concentrations of As(aq), as As(III), increased in the pore-water. With the release of As in the suboxic zones Sb partitions into the solid phase, possibly occupying sorption sites previously occupied by As(V).

The inherent stability of the Sb(V)–O solid-phase is indicated by (1) a consistent proportion of total Sb under differing redox conditions, and (2) the persistence of this phase over time and in response to gradual burial and a decrease in oxygen with depth. This stability could be caused by strong sorption, Sb mineral precipitation or Sb incorporation into an iron oxide phase. The persistence of the Sb(V)–O phase under reducing conditions at BP and at BCV suggests strong surface complexes on the surfaces of Fe-oxides (Ackermann et al., 2008; Leuz et al., 2006a; Mitsunobu et al., 2006), or the occupation of different mineral sites. For example, Mitsunobu et al. (2010) found that Sb(V) was incorporated into the structure of ferrihydrite, goethite, and natural Fe(III)-oxides during co-precipitation studies and was therefore not greatly influenced by changes in aquatic factors. Alternatively, the sequestration of Sb may also be explained by the formation of Sb minerals, where comparable minerals are not formed in the As system. Tripuhyite ($FeSbO_4$), schafarzite ($FeSb_2O_4$), $Ca_2Sb_2O_7$, and $Pb_2Sb_2O_7$ have been identified as the primary controls on Sb mobility in mine wastes rich in Sb (Majzlan, 2008; Leverett et al., 2012; Diemar et al., 2009) and have been extensively characterized (i.e. Lalinská-Voleková et al., 2012). It was determined that, once formed, these structures are relatively insoluble. Equivalent As minerals have not been identified.

The reason for the co-existence of the reduced As species and the oxidized Sb species in pore-water, forever, requires further explanation. Arsenic(III) and Sb(V) co-exist in pore-water at BP, BCC, and BCV. The co-existence of As(III) and Sb(V) in pore-water and surface water has been observed by other researchers as well (Casiot et al., 2007; Mitsunobu et al., 2006; Mok and Wai, 1990). Currently, there exist few reliable thermodynamic data for Sb and the data that do exist for As and Sb often are not calculated for comparable species. The standard electrode potentials for the reduction of H_3AsO_4 to H_3AsO_3 and $Sb(OH)_6^-$ to $Sb(OH)_3$ have been calculated to be 0.56 and 0.76, respectively (Wilson et al., 2010 and references therein) suggesting that as porewaters undergo reduction Sb should reduce before As. It has already been mentioned that the aqueous As(III) oxidation rate is much faster than the Sb(III) rate and presumably the reduction rate is also much faster for As than for Sb. However, the oxidized form of each species is not comparable and other thermodynamic data indicate the reverse for these two elements. To account thermodynamically for the co-existence of As(III) and Sb(V), given the narrow range of pH values in pore-water, the redox conditions of the system must be within a relatively narrow range, assuming equilibrium. For example, if As(III) and Sb(V) co-exist at all three sites, all the sites must exhibit similar redox conditions, that is, their redox potentials all lie within the same narrow range. This scenario is unlikely given that BP has elevated SO_4^{2-}, lower Fe(II), and a complete lack of vegetation, compared to BCV. Furthermore, the BCV samples give off a distinctive H_2S smell, which is produced only under more reducing conditions (Stumm and Morgan, 1996). Based on these observations, BCV appears to have a much lower oxidation potential compared to BP. Yet, Sb(V) persists as the dominant species at both sites. Therefore, other factors controlling aqueous Sb speciation must be considered.

Precipitation or adsorption of the Sb(III)–S phase may be preferentially removing Sb(III) from pore-water, leaving only the Sb(V) species. Antimony(III) bound to S was present in the ore as stibnite and sulfosalts, but these Sb ore minerals were completely converted in the roaster (Fawcett and Jamieson, 2011). Also, in micro-XANES and micro-XRD studies by Fawcett and Jamieson (2011) found that the Sb(III)–S phase is associated with the maghemite and hematite iron oxides suggesting a destabilization of Sb bound to the roaster oxide and a reprecipitation or sorption onto secondary sulfides (visible in thin section). The conversion of the primary Sb-sulfide in the roaster, the proximal association of the identified Sb(III)–S phase to the primary Sb host in roaster waste, and its appearance only in the more reduced portions of the profile suggest that the Sb(III)–S phase is formed in sediment. Arsenic(III) bound to S was not present in the ore; consequently, where found at depth in the downstream sediments must also represent a secondary phase. These phases could result from As and Sb adsorbing to the surface of a sulfide, such as mackinawite and pyrite (Farquhar et al., 2002; Gallegos et al., 2007; Kirsch et al., 2008; Wolthers et al., 2007), or from the precipitation of an As(III) and Sb(III) sulfide phase (Farquhar et al., 2002; La Force et al., 2000; Kirsch et al., 2008; Moore et al., 1988; Newman et al., 1997).

The distributions of the As(III)–S and Sb(III)–S phases at BCV indicate that they are not stable when exposed to higher O_2 levels and lower pH. A peak in concentrations of aqueous As and Sb at −10 cm occurs within the root zone, or rhizosphere, which is where interactions between the sediment and plant roots take place (Lombi and Nolan, 2005). Rhizosphere geochemistry often differs from that of the bulk soil or sediment, mainly because of greater acidity (Lombi and Nolan, 2005; Kirk et al., 1993). The transfer of O_2 from the root to the surrounding soil leads to the oxidation of sulfides and the generation of H^+ ions (Kirk and Bajita, 1995). Similar to lowland rice, horsetails have deep and extensive root systems (Brooks et al., 1981). A decrease in pH of 1.3 units is observed in sediments between −10 and −12 cm depth at BCV (Fig. 4), which is similar to pH declines observed in the lowland rice rhizosphere (Kirk and Bajita, 1995). Within the same zone there is a peak in pore-water concentrations of As, Sb, and S^{2-}. An oxygen influx from the roots to the sediments appears to be oxidizing the secondary As and Sb S-bound phases and causing acidification of the rhizosphere; thus mobilizing Sb, As, and S^{2-}. This assessment is supported by solid-state speciation results, which indicate Sb(V)–O constitutes a greater percentage of the Sb solid-phase over the root zone, and an Sb(III)–S phase is present above and below, but not within the narrow interval corresponding to the root zone.

The main factors that differentiate the sites, and hence may explain the relative mobilities of As and Sb, are redox conditions and the presence of vegetation. Data and observations suggest that conditions at BCV are more reducing than at BP and precipitation of As and Sb as sulfides may be occurring. Also, As and Sb are associated with horsetails in BCV, as evident by the elevated concentrations of As and Sb associated with the two plants collected, and the association of As and Sb with organic matter in the vegetated zone and not in the deeper zones. Plant-related processes can effectively attenuate metal(loid)s (Lombi and Nolan, 2005; Buschmann and Sigg, 2004; Lintschinger et al., 1998; Stollenwerk, 2003; Violante et al., 2005; Slowey et al., 2007). The presence of vegetation may be a factor responsible for the lowered mobility of As and Sb in BCV.

5. Implications for remediation

A complex remediation plan has been developed for the Giant Mine site which would reduce but not eliminate the loading of dissolved As to Baker Creek (INAC, 2007). The "developer" of the site is identified as the Giant Mine Remediation Directorate, which involves both the federal and territorial governments. As a result, the entire submission, including approximately 50 consultants' reports, is available to researchers. The Mackenzie Valley Environmental Impact Review Board, which is the regulatory body in the Northwest Territories, responded in June 2013 to the proposed remediation plan, and recommended 26 measures, or modifications and additions to the remediation plan (MVRB, 2013). In August 2014, the plan was approved by the federal government of Canada with some rewording of the recommendations from the regulatory board. The complexity of the site, the amount of technical information gathered, the requirement to involve other parties, notably the local First Nations communities and NGOs (Non-Governmental Organizations), and the nature of the environmental assessment process have all contributed to the long timeline and large volume of documentation (Jamieson, 2014). Within the remediation plan, and the regulator's response, there is acknowledgement that Sb contamination was associated with As, and that guidelines for Sb are exceeded where those exist. However, there is little focus on remediation measures for contaminants other than As, the assumption being that the risk from exposure to As is the most serious concern, and that remediation of high-As materials will likely lower concentrations of other elements of concern.

Baker Creek, the location of the three sample site in this study, is an important part of the Giant Mine remediation plan since the creek flows through the mine property and provides one of the routes whereby dissolved As and Sb are discharged into Great Slave Lake, and contains contaminated sediments and vegetation. There are several options for Baker Creek, including diversion and sediment removal.

The research reported in this paper was conducted in parallel with the remediation plan, and offers several results that were not covered in previous studies and have direct implications for remediation options:

(1) The distribution of As and Sb sediment and pore water concentrations with depth (Fig. 6) indicates that sediments continue to be a source of these elements to the overlying surface water. For both BCC and BCV, it is clear that As- and Sb-enriched pore water is migrating upwards from highly contaminated buried sediments, which are the legacy of spills in the past. This phenomenon will continue even if other sources of As and Sb to Baker Creek, such as discharge from the water treatment plant, or leaching from contaminated soils adjacent to the creek bed, are reduced.

(2) Aquatic vegetation has an important effect on the mobility of As and Sb. Historically, the proliferation of horsetails behind the barrier constructed at the outlet of Baker Creek trapped the particularly As- and Sb-rich fine particles released by spills and tailings pond decants, resulting in much higher sediment concentrations of these contaminants compared with the main creek channel. The horsetails have taken up As and Sb and possibly introduced the contaminants into the food chain. If remediation involves removal of sediments in the outlet area, both the fine sediments and the horsetails should be included.

6. Conclusions

It is evident that As and Sb exhibit some differences in geochemical behavior. The Sb(V)–O phase is more stable than the As(V)–O phase over a wide range of redox conditions, consistent with results reported by Mitsunobu et al. (2006). Furthermore, Sb is well attenuated in reducing environments and at all depths when As and Sb loading is relatively low. In contrast, As is relatively mobile in reducing environments and is more readily attenuated in the surficial zone. Finally, the oxidized species of Sb and the reduced species of As dominate the pore-waters in the reduced zones. Contrary to what may be predicted based on the aqueous speciation alone, Sb is undergoing post-depositional changes, but unlike As, the cycling of Sb may involve the preferential partitioning of the reduced species to the solid phase or controlled by a pyrochlore mineral phase unique to the Sb system. This highlights the importance of studying both the aqueous and solid-phase speciation.

Research into the mobility of Sb in mining environments is becoming more prevalent. However, in order to understand the geochemical behavior of this element, reliable thermodynamic data, most notably for the oxyanion equivalents of As, are needed. Furthermore, the adsorption dynamics and relative affinities of As and Sb on different mineral surfaces should be directly compared in studies as these elements are often associated in the environment and may compete for sorption sites. Given this information the relative mobility of co-existing As and Sb could be more accurately predicted.

Acknowledgements

PNC/XOR facilities at the Advanced Photon Source, and research at these facilities, are supported by the U.S. Department of Energy – Basic Energy Sciences, a major facilities access grant from NSERC, the University of Washington, Simon Fraser University and the Advanced Photon Source. Use of the Advanced Photon Source is also supported by the U.S. Department of Energy, Office of Science, Office of Basic Energy Sciences, under Contract DE-AC02-06CH11357. This study was partly funded through the NSERC Northern Research Internship and by the Mineralogical Association of Canada. We thank the Giant Mine Remediation Team for site access and kindly support, and Robert Gordon for the many hours of beamline assistance. The use of trade or brand names is for identification purposes only, and does not constitute endorsement by the U.S. Geological Survey.

References

Ackermann, S., Majzlan, J., Bolanz, R., Giere, R., Newville, M., 2008. Sb sorption complexes on Fe oxide surfaces: an EXAFS study. Geochim. Cosmochim. Acta 72. A5.

Andrade, C.F., Jamieson, H.E., Kyser, T.K., Praharaj, T., Fortin, D., 2010. Biogeochemical redox cycling of As in mine-impacted lake sediments and co-existing pore-waters near Giant mine, Yellowknife Bay, Canada. Appl. Geochem. 25, 199–211.

Appelo, C.A.G., Postma, D., 2005. Geochemistry, Groundwater and Pollution. Balkema, Amsterdam, The Netherlands.

Ashley, P.M., Craw, D., Graham, B.P., Chappell, D.A., 2003. Environmental mobility of antimony around mesothermal stibnite deposits, New South Wales, Australia and southern New Zealand. J. Geochem. Explor. 77, 1–14.

Asryan, N.A., Alikhanyan, A.S., Nipan, G.D., 2003. Thermodynamic stability of antimony oxides. Russ. J. Phys. Chem. 78, 5–11.

Asta, M.P., Nordstrom, D.K., McCleskey, R.B., 2012. Simultaneous oxidation of arsenic and antimony at low and circumneutral pH, with and without microbial catalysis. Appl. Geochem. 27, 281–291.

Banfield, J.F., Nealson, K.H., 1997. Geomicrobiology: Interactions between Microbes and Minerals. Mineralogical Society of America Geochemical Society, Washington, DC.

Barringer, J.L., Johnsson, P.A., 1989. Theoretical Considerations and a Simple Method for Measuring Alkalinity and Acidity in Low-pH Waters by Gran Titration. U.S. Geological Survey, Water-Resour. Invest. Report 89-4029.

Belzile, N., Chen, Y., Wang, Z., 2001. Oxidation of antimony (III) by amorphous iron and manganese oxyhydroxides. Chem. Geol. 174, 379–387.

Bertine, K.K., Lee, D.S., 1983. Antimony content and speciation in the water column and interstitial waters of Saanich Inlet. In: Wong, C.S., Boyle, E., Bruland, K.W., Burton, J.D., Goldberg, E.D. (Eds.), Trace Metals in Sea Water. NATO Adc. Res. Inst. Plenum, New York, USA, pp. 21–38.

Berube, Y., Frenette, M., Gilbert, R., Anctil, C., 1974. Studies of Mine Waste Containment at Two Mines near Yellowknife, NWT, ALUR 1972-73. QS-3038-000-EE-A1, pp. 1–181.

Bowell, R.J., 1994. Sorption of arsenic by iron-oxides and oxyhydroxides in soils. Appl. Geochem. 9, 279–286.

Brinton, T.I., Antweiler, R.C., Taylor, H.E., 1995. Method for the Determination of Dissolved Chloride, Nitrate, and Sulfate in Natural Water Using Ion Chromatography. U.S. Geol. Survey Open-File Report 95-426A.

Brooks, R.R., Holzbecher, J., Ryan, D.E., 1981. Horsetails (equisetum) as indirect indicators of gold mineralization. J. Geochem. Explor. 16, 21–26.

Buschmann, J., Sigg, L., 2004. Antimony(III) binding to humic substances: influence of pH and type of humic acid. Environ. Sci. Technol. 38, 4535–4541.

Canam, T.W., 2006. Discover, mine production, and geology of the giant mine. In: Anglin, C.D., Falck, H., Wright, D.F., Ambrose, E.J. (Eds.), Gold in the Yellowknife Greenstone Belt, Northwest Territories: Results of the EXTECH III Multidisciplinary Research Project. Geological Association of Canada-Mineral Deposits Division, St. John's, Newfoundland & Labrador, Canada, p. 196.

Casiot, C., Ujevic, M., Munoz, M., Seidel, J.L., Elbaz-Poulichet, F., 2007. Antimony and arsenic mobility in a creek draining an antimony mine abandoned 85 years ago (upper Orb basin, France). Appl. Geochem. 22, 788–798.

Chen, Y., Deng, T., Filella, M., Belzile, N., 2003. Distribution and early diagenesis of antimony species in sediments and porewaters of freshwater lakes. Environ. Sci. Technol. 37, 1163–1168.

Cherry, J.A., Shaikh, A.U., Tallman, D.E., Nicholson, R.V., 1979. Arsenic species as an indicator of redox conditions in groundwater. J. Hydrol. 43, 373–392.

Coleman, L.C., 1957. Mineralogy of the Giant Yellowknife Gold Mine, Yellowknife, NWT. Econ. Geol. 52, 400–425.

Connor, B.F., Currier, J.P., Woodworth, M.T., 2001. Results of the U.S. Geological Survey's Analytical Evaluation Program for Standard Reference Samples Distributed in October 2000. U.S. Geol. Survey Open-File Report 01-137, 116 p.

Craigen, M.C., 2006. Controls on Arsenic Speciation in Mine Tailings and Co-existing Pore Water in Freshwater and Marine Settings from the Lower Seal Harbour Gold District, Nova Scotia, Canada. M.Sc. Thesis, Queen's University.

Diemar, G.A., Filella, M., Leverett, P., Williams, P.A., 2009. Dispersion of antimony from oxidizing ore deposits. Pure Appl. Chem. 81 (9), 1547–1553.

Dixit, S., Hering, J.G., 2003. Comparison of Arsenic (V) and Arsenic (III) sorption onto iron oxide minerals: implications for arsenic mobility. Environ. Sci. Technol. 37, 4182–4189.

Eary, L.E., Schramke, J.A., 1990. Rates of inorganic oxidation reactions involving dissolved-oxygen. Am. Chem. Soc. Symp. Ser. 416, 379–396.

Ehrlich, H.L., 2002. Geomicrobiology, fourth ed. Marcel Dekker, New York, 768 p.

Farrar, J.W., 2000. Results of the U.S. Geological Survey's Analytical Evaluation Program for Standard Reference Samples Distributed in October 1999. U.S. Geol. Survey Open-File Report 00-227, 143 p.

Farquhar, M.L., Charnock, J.M., Livens, F.R., Vaughan, D.J., 2002. Mechanisms of arsenic uptake from aqueous solution by interaction with goethite, lepidocrocite, mackinawite, and pyrite: an X-ray absorption spectroscopy study. Environ. Sci. Technol. 36, 1757–1762.

Fawcett, S.E., Andrade, C.F., Walker, S.R., Jamieson, H.E., 2006. Understanding the environmental legacy of the Giant gold mine, Yellowknife, NWT: lessons from recent research. In: Proceedings of CLRA/ACRSD 2006 Annual Meeting, Reclamation and Remediation: Policy to Practice, August 20–23, Ottawa, Canada.

Fawcett, S.E., Gordon, R.A., Jamieson, H.E., 2010. Optimizing experimental design, overcoming challenges, and gaining valuable information from the Sb K-edge XANES region. Am. Mineral. 94, 1377–1387.

Fawcett, S., Jamieson, H., 2011. The distinction between ore processing and post depositional transformation on the speciation of As and Sb in mine waste and sediment. Chem. Geol. 283, 109–118.

Filella, M., Belzile, N., Chen, Y., 2002. Antimony in the environment: a review focused on natural waters: II. Relevant solution chemistry. Earth-Sci. Rev. 59, 265–285.

Fillela, M., Blezile, N., Lett, M.-C., 2007. Antimony in the environment: a review focused on natural waters. III. Microbiota relevant reactions. Earth-Sci. Rev. 80, 195–217.

Gallegos, T.J., Hyun, S.P., Hayes, K.F., 2007. Spectroscopic investigation of the uptake of arsenite from solution by synthetic mackinawite. Environ. Sci. Technol. 41, 7781–7786.

Giant Yellowknife Mines Limited, 1981. A Submission to the Northwest Territories Water Board.

Glew, J., 1989. A new trigger mechanism for sediment core sampling. J. Paleolimnol. 2, 241–243.

Greenwood, N.N., Earnshaw, A., 1984. Arsenic, antimony, bismuth. In: Greenwood, N.N. (Ed.), Chemistry of the Elements. Pergamon Press, London, pp. 547–578.

Heald, S.M., Cross, J.O., Brewe, D.L., Gordon, R.A., 2007. The PNC/XOR X-ray microprobe station at APS sector 20. Nucl. Instrum. Methods A 582, 215–217.

Hozhina, E.I., Khramov, A.A., Gerasimov, P.A., Kumarkov, A.A., 2001. Uptake of heavy metals, arsenic, and antimony by aquatic plants in the vicinity of ore mining and processing industries; geochemical studies of mining and the environment. J. Geochem. Explor. 74, 153–162.

INAC (Indian and Northern Affairs Canada), 2007. Giant Mine Remediation Plan. Report of the Giant Mine Remediation Team-Department of Indian Affairs and Northern Development as submitted to the Mackenzie Valley Land and Water Board, Yellowknife, Canada, 2007, 260 pp.

Inskeep, W.P., McDermott, T.R., Fendorf, S., 2002. Arsenic (V)/(III) cycling in soils and natural waters: chemical and microbiological processes. In: Frankenberger, W.T.J. (Ed.), Environmental Chemistry of Arsenic. Marcel Dekker Inc., New York, NY, pp. 183–215.

Jamieson, H., 2014. The legacy of arsenic contamination from mining and processing refractory gold ore at Giant Mine, Yellowknife, Northwest Territories, Canada. Rev. Mineral. Geochem. 79, 533–553.

Jamieson, H.E., Walker, S.R., Andrade, C.F., Rasmussen, P., Beauchemin, S., Lanzirotti, A., Parsons, M.B., Wrye, L.A., 2011. Direct identification of metal compounds in contaminated soil, mine tailings, lake sediments and house dust using synchrotron-based microanalysis. Hum. Ecol. Risk Assess. 17, 1292–1309.

Kirk, G.J.D., Bajita, J.B., 1995. Root-induced iron oxidation, Ph changes and zinc solubilization in the rhizosphere of lowland rice. New Phytol. 131, 129–137.

Kirk, G.J.D., Begg, C.B.M., Solivas, J.L., 1993. The chemistry of the lowland rice rhizosphere. Plant Soil 156, 83–86.

Kirsch, R., Scheinost, A.C., Rossberg, A., Banerjee, D., Charlet, L., 2008. Reduction of antimony by nano-particulate magnetite and mackinawite. Mineral. Mag. 72, 185–189.

Kneebone, P.E., O'Day, P.A., Jones, N., Hering, J.G., 2002. Deposition and fate of arsenic in iron- and arsenic-enriched reservoir sediments. Environ. Sci. Technol. 36, 381–386.

Krupka, K.M., Serne, R.J., 2002. Geochemical Factors Affecting the Behaviour of Antimony, Cobalt, Europium, Technetium, and Uranium in Vadose Sediments. PNNL-14126.

Kuehnelt, D., Goessler, W., Irgolic, K.J., 1997. The oxidation of arsenite in aqueous solutions. In: Abernathy, C.O., Claderone, R.L., Chappelle, W.R. (Eds.), Arsenic: Exposure and Health Effects. Chapman and Hall, London, pp. 45–54 (Chapter 4).

La Force, M.J., Hansel, C.M., Fendorf, S., 2000. Arsenic speciation, seasonal transformations, and co-distribution with iron in a mine waste-influenced palustrine emergent wetland. Environ. Sci. Technol. 34, 3937–3943.

Lalinská-Voleková, B., Majzlan, J., Klimko, T., Chovan, M., Kučerová, G., Michňová, J., Hovorič, R., Göttlicher, J., Steininger, R., 2012. Mineralogy of weathering products of Fe–As–Sb mine wastes and soils at several Sb deposits in Slovakia. Can Mineral. 50, 481–500.

Langmuir, D., 1997. Aqueous Environmental Geochemistry. Prentice-Hall, Upper Saddle River, NJ.

Leverett, P., Reynolds, J.K., Roper, A.J., Williams, P.A., 2012. Tripuhyite and schafarzikite: two of the ultimate sinks for antimony in the natural environment. Mineral. Mag. 76, 891–902.

Leuz, A.K., Monch, H., Johnson, C.A., 2006a. Sorption of Sb(III) and Sb(V) to goethite: Influence on Sb(III) oxidation and mobilization. Environ. Sci. Technol. 40, 7277–7282.

Leuz, A., Hug, S.J., Wehrli, B., Johnson, C.A., 2006b. Iron-mediated oxidation of antimony(III) by oxygen and hydrogen peroxide compared to arsenic(III) oxidation. Environ. Sci. Technol. 40, 2565–2571.

Lintschinger, J., Michalke, B., Schulte-Hostede, S., Schramel, P., 1998. Studies on speciation of antimony in soil contaminated by industrial activity. Int. J. Environ. Anal. Chem. 72, 11–25.

Lombi, E., Nolan, A.L., 2005. Metal and arsenic bioavailability and uptake by hyperaccumulator plants. In: Shtangeeva, I. (Ed.), Trace and Ultratrace Elements in Plants and Soil. WIT Press, Great Britain, pp. 97–128.

Majzlan, J., 2008. Stabilization of iron oxide nanoparticles by the adsorption of sulfate, phosphate and arsenate. Geochim. Cosmochim. Acta 72. A587.

Manning, B.A., Fendorf, S.E., Goldberg, S., 1998. Surface structures and stability of arsenic(III) on goethite: spectroscopic evidence for inner-sphere complexes. Environ. Sci. Technol. 32, 2383–2388.

Manning, B.A., Fendorf, S.E., Bostick, B., Suarez, D.L., 2002. Arsenic(III) oxidation and arsenic(V) adsorption reactions on synthetic birnessite. Environ. Sci. Technol. 36, 976–981.

Marsden, J.O., House, C.I., 2006. The Chemistry of Gold Extraction. Society for Mining, Metallurgy, and Exploration, Inc., USA.

Martin, A.J., Pedersen, T.F., 2002. Seasonal and inter-annual mobility of As in a lake impacted by metal mining. Environ. Sci. Technol. 36, 1516–1523.

Martinez-Llado, X., de Pablo, J., Gimenez, J., Ayora, C., Marti, V., Rovira, M., 2008. Sorption of antimony (V) onto synthetic goethite in carbonate medium. Solv. Extract. Ion Exch. 26, 289–300.

McCleskey, D.K., Nordstrom, D.K., Ball, J.W., 2001. Cation-exchange separation of interfering metals from acid mine waters for accurate determination of total arsenic and arsenic(III) by hydride generation-atomic absorption spectrometry. 43rd Rocky Mountain Conference on Analytical Chemistry, Denver, CO, July 29–Augusts 2.

McCleskey, R.B., Nordstrom, D.K., Maest, A.S., 2004. Preservation of water samples for arsenic(III). Appl. Geochem. 19, 995–1009.

McQuiston, F.W.J., Shoemaker, R.S., 1975. Gold and Silver Cyanidation Plant Practices Monograph. The American Institute of Mining, Metallurgical, and Petroleum Engineers, Inc. Port City Press, MD, USA.

Milham, L., Craw, D., 2009. Antimony mobilization through two contrasting gold ore processing systems, New Zealand. Mine Water Environ. 28, 136–145.

Mitsunobu, S., Harada, T., Takahashi, Y., 2006. Comparison of antimony behavior with that of arsenic under various soil redox conditions. Environ. Sci. Technol. 40, 7270–7276.

Mitsunobu, S., Takahashi, Y., Terada, Y., Sakata, M., 2010. Antimony (V) incorporation into synthetic ferrihydrite, goethite, and natural iron oxides. Environ. Sci. Technol. 44, 3712–3718.

Mok, W.M., Wai, C.M., 1990. Distribution and mobilization of arsenic and antimony species in the Coeur-Dalene River, Idaho. Environ. Sci. Technol. 24, 102–108.

Moore, J.N., Ficklin, W.H., Johns, C., 1988. Partitioning of arsenic and metals in reducing sulfidic sediments. Environ. Sci. Technol. 22, 432–437.

More, M.A., Pawson, H.E., 1978. Giant Yellowknife Mines Limited. In: Pickett, D.E. (Ed.), Milling Practice in Canada, pp. 63–65.

Morin, G., Ostergren, J.D., Juillot, F., Ildefonse, P., Calas, G., Brown, G.E., 1999. XAFS determination of the chemical form of lead in smelter-contaminated soils and mine tailings: importance of adsorption processes. Am. Mineral. 84, 420–434.

MVRB (Mackenzie Valley Review Board), 2013. Report of Environmental Assessment and Reasons for Decision, Giant Mine Remediation Project EA0809-001, 245 p.

Newman, D.K., Beveridge, T.J., Morel, F.M.M., 1997. Precipitation of arsenic trisulfide by Desulfotomaculum auripigmentum. Appl. Environ. Microbiol. 63, 2022–2028.

Nishimura, T., Umetsu, Y., 2000. Chemistry on elimination of arsenic, antimony and selenium from aqueous solutions with iron(III) species. In: Young, C.A. (Ed.), Minor Metals 2000. SME, Littleton, CO, pp. 105–112.

Nordstrom, D.K., 2003. Effects of microbiological and geochemical interactions in mine drainage. In: Jambor, J.L., Blowes, D.W., Ritchie, A.I.M. (Eds.), Environmental Aspects of Mine Wastes. Mineral. Assoc. Canada Short Course, vol. 31, pp. 227–238.

Nordstrom, D.K., Campbell, K.M., 2013. Modeling low-temperature geochemical processes. In: Drever, J.I. (Ed.), Surface and Groundwater, Weathering and Soils. Elsevier, New York, pp. 27–68.

Nordstrom, D.K., Munoz, J.L., 1994. Geochemical Thermodynamics. Blackwell Scientific Publications, Boston.

Pierce, M.L., Moore, C.B., 1982. Adsorption of arsenite and arsenate on amorphous iron hydroxide. Water Res. 16, 1247–1253.

Riveros, P.A., Dutrizac, J.E., Chen, T.T., 2000. Recovery of Marketable Arsenic Trioxide from Arsenic-Rich Roaster Dust. Environmental Improvements in Mineral Processing and Extractive Metallurgy, vol. II, pp. 135–149.

Scheinost, A.C., Rossberg, A., Vantelon, D., Xifra, I., Kretzschmar, R., Leuz, A.K., Funke, H., Johnson, C.A., 2006. Quantitative antimony speciation in shooting-range soils by EXAFS spectroscopy. Geochim. Cosmochim. Acta 70, 3299–3312.

Sigg, L., 2000. Redox potential measurements in natural waters: significance: concepts and problems. In: Schuring, J., Schulz, H.D., Fischer, W.R., Bottcher, J., Duijnisveld, W.H.M. (Eds.), Redox: Fundamentals, Processes and Applications. Springer, Berlin.

Slowey, A.J., Johnson, S.B., Newville, M., Brown, G.E., 2007. Speciation and colloid transport of arsenic from mine tailings. Appl. Geochem. 22, 1884–1898.

Stollenwerk, K.G., 2003. Geochemical processes controlling transport of arsenic in groundwater: a review of adsorption. In: Welch, A.H., Stollenwerk, K.G. (Eds.), Arsenic in Ground Water Geochemistry and Occurence. Kluwer Academic Publishers, USA, pp. 67–100.

Stolz, J.F., Basu, P., Santini, J.M., Oremland, R.S., 2006. Arsenic and selenium in microbial metabolism. Annu. Rev. Microbiol. 60, 107–130.

Stookey, L.L., 1970. FerroZine—a new spectrophotometric reagent for iron. Anal. Chem. 42, 779–781.

Stumm, W., Morgan, J.J., 1996. Aquatic Chemistry. John Wiley & Sons Inc., New York, USA.

Takahashi, T., Shozugawa, K., Matsuo, M., 2010. Contribution of amorphous iron compounds to adsorptions of pentavalent antimony in soils. Water Air Soil Pollut. 208, 165–172.

To, T.B., Nordstrom, D.K., Cunningham, K.M., Ball, J.W., McCleskey, R.B., 1999. New method for the direct determination of dissolved Fe(III) concentration in acid mine waters. Environ. Sci. Technol. 33, 807–813.

Violante, A., Ricciardella, M., Pigna, M., Capasso, R., 2005. Effects of organic ligands on the adsorption of trace elements onto metal oxides and organo-mineral complexes. In: Huang, P.M., Gobran, G.R. (Eds.), Biogeochemistry of Trace Elements in the Rhizosphere. Elsevier B.V., Amsterdam, The Netherlands, pp. 157–182.

Walker, S.R., Jamieson, H.E., Lanzirotti, A., Andrade, C.F., Hall, G.E.M., 2005. The speciation of arsenic in iron oxides in mine wastes from the Giant gold mine, NWT: application of synchrotron micro-XRD and micro-XANES at the grain scale. Can. Mineral. 43, 1205–1224.

Walker, S.R., Jamieson, H.E., Lanzirotti, A., Hall, G.E.M., Peterson, R.C., 2015. The effect of ore roasting on arsenic oxidation state and solid phase speciation in gold mine tailings. Geochem.: Explor. Environ. Anal., in press.

Watkins, R., Weiss, D., Dubbin, W., Peel, K., Coles, B., Arnold, T., 2006. Investigations into the kinetics and thermodynamics of Sb(III) adsorption on goethite (alpha-FeOOH). J. Colloid Interface Sci. 303, 639–646.

Waychunas, G.A., Rea, B.A., Fuller, C.C., Davis, J.A., 1993. Surface-chemistry of ferrihydrite. 1. Exafs studies of the geometry of coprecipitated and adsorbed arsenate. Geochim. Cosmochim. Acta 57, 2251–2269.

Wilson, S., Lockwood, P., Ashley, P., Tighe, M., 2010. The chemistry and behaviour of antimony in the soil environment with comparisons to arsenic: a critical review. Environ. Pollut. 158, 1169–1181.

Wolthers, M., Butler, I.B., Rickard, D., 2007. Influence of arsenic on iron sulfide transformations. Chem. Geol. 236, 217–227.